Published in final edited form as:
Heart Rhythm. 2012 May ; 9(5): 760–769. doi:10.1016/j.hrthm.2011.12.006.

A Novel Rare Variant in *SCN1Bb* Linked to Brugada Syndrome and SIDS by Combined Modulation of $Na_v1.5$ and $K_v4.3$ Channel Currents

Dan Hu, MD, PhD[1,#], **Hector Barajas-Martínez, PhD**[1,#], **Argelia Medeiros-Domingo, MD, PhD**[2,#], **Lia Crotti, MD, PhD**[3,4,5,#], **Christian Veltmann, MD**[6], **Rainer Schimpf, MD**[6], **Janire Urrutia, PhD**[7], **Aintzane Alday, PhD**[7], **Oscar Casis, MD, PhD**[7], **Ryan Pfeiffer, BS**[1], **Elena Burashnikov, BS**[1], **Gabriel Caceres, BS**[1], **David J. Tester, BS**[2], **Christian Wolpert, MD**[8], **Martin Borggrefe, MD**[6], **Peter Schwartz, MD**[3,5,9,10,11,12], **Michael J. Ackerman, MD, PhD**[2], and **Charles Antzelevitch, PhD, FHRS**[1,*]

[1]Masonic Medical Research Laboratory, Utica, New York, United States of America

[2]Windland Smith Rice Sudden Death Genomics Laboratory, Mayo Clinic, Rochester, Minnesota, United States of America

[3]Department of Lung, Blood and Heart, Section of Cardiology, University of Pavia, Pavia, Italy

[4]Institute of Human Genetics, Helmholtz Zentrum Muenchen, Neuherberg, Germany

[5]Department of Cardiology, IRCCS Policlinico S. Matteo, Pavia, Italy

[6]University Medical Centre Mannheim, Mannheim, Germany

[7]Universidad del País Vasco, Department of Physiology, Leioa, Spain

[8]Klinikum Ludwigsburg, Ludwigsburg, Germany

[9]Laboratory of Cardiovascular Genetics, IRCCS Istituto Auxologico Italiano, Milan, Italy

[10]Cardiovascular Genetics Laboratory, Hatter Institute for Cardiovascular Research, Department of Medicine, University of Cape Town, South Africa

[11]Department of Medicine, University of Stellenbosch, South Africa

[12]Chair of Sudden Death, Department of Family and Community Medicine, College of Medicine, King Saud University, Riyadh, Saudi Arabia

Abstract

[*]Address for editorial correspondence and reprint requests: Charles Antzelevitch, PhD., FAHA, FACC, FHRS, Gordon K. Moe Scholar, Masonic Medical Research Laboratory, 2150 Bleecker Street, Utica, New York, U.S.A. 13501-1787, Phone: (315) 735-2217, FAX: (315) 735-5648, ca@mmrl.edu.
[#]Authors contributed equally

CONFLICT OF INTEREST STATEMENT

Michael J. Ackerman is a consultant for Transgenomic and their FAMILION™ genetic test for cardiac ion channel abnormalities. In addition, “cardiac channel gene screen” and “know-how relating to long QT genetic testing” license agreements, resulting in consideration and royalty payments, were established between Genaissance Pharmaceuticals (then PGxHealth and now Transgenomic, Omaha, Neb) and Mayo Medical Ventures (now Mayo Clinic Health Solutions, Rochester, Minn) in 2004. However, Transgenomic did not provide financial support for this study. The other authors have no financial or other considerations to disclose.

BACKGROUND—Cardiac sodium channel β-subunit mutations have been associated with several inherited cardiac arrhythmia syndromes.

OBJECTIVE—To identify and characterize variations in *SCN1Bb* associated with Brugada (BrS) and sudden infant death syndromes (SIDS).

METHODS AND RESULTS—Patient 1 was a 44-y/o male with an ajmaline-induced Type-1 ST-segment elevation in V1 and V2 supporting the diagnosis of BrS. Patient 2 was a 62-y/o female displaying a coved-type BrS ECG who developed cardiac arrest during fever. Patient 3 was a 4-m/o female SIDS case. All known exons and intron borders of BrS and SIDS susceptibility genes were amplified and sequenced in both directions. A R214Q variant was detected in exon 3A of *SCN1Bb* ($Na_v\beta1B$) in all three probands, but not in any other gene previously associated with BrS or SIDS. R214Q was identified in 4 of 807 ethnically-matched healthy controls (0.50%). Wild type (WT) and mutant genes were expressed in TSA201 cells and studied using whole-cell patch-clamp and co-immunoprecipitation techniques. Co-expression of *SCN5A*/WT+*SCN1Bb*/R214Q resulted in peak sodium channel current (I_{Na}) 56.5% smaller compared to *SCN5A*/WT+*SCN1Bb*/WT (n=11–12, p<0.05). Co-expression of *KCND3*/WT+*SCN1Bb*/R214Q induced a Kv4.3 current (I_{to}) 70.6% greater compared with *KCND3*/WT+*SCN1Bb*/WT(n=10–11, p<0.01). Co-immunoprecipitation indicated structural association between $Na_v\beta1B$ and $Na_v1.5$ and $K_v4.3$.

CONCLUSION—Our results suggest that R214Q variation in *SCN1Bb* is a functional polymorphism that may serve as a modifier of the substrate responsible for Brugada or SIDS phenotypes via a combined loss of function of I_{Na} and gain of function of I_{to}.

Keywords

Brugada Syndrome; Sudden Infant Death Syndrome; Arrhythmias; SCN1Bb; Sodium; Potassium

INTRODUCTION

Brugada syndrome (BrS) is an inherited cardiac arrhythmia disease characterized by an ST-segment elevation in the right precordial electrocardiogram (ECG) leads and a high incidence of sudden cardiac death (SCD). Reported in both children and the elderly, it is more common in males than females and typically first presents in the third or fourth decade of life.[1] BrS has been associated with genetic variants in 11 different genes (*SCN5A, GPD1L, CACNA1C, CACNB2b, SCN1B, KCNE3, SCN3B, KCNJ8, CACNA2D1, KCND3* and *MOG1*).[2–5] Approximately 60% of BrS probands remain genotype-negative.

Sudden infant death syndrome (SIDS) is characterized by the sudden death of an infant (<1 y/o) that remains unexplained despite thorough examination. It is a major contributor to post-neonatal infant death, and is the third leading cause of infant mortality in USA.[6] Over the past decade, postmortem genetic analysis or molecular autopsies of SIDS cases have identified a number of cardiac ion channel mutations associated with arrhythmia syndromes, including BrS, long QT syndrome (LQTS), short QT syndrome (SQTS), and catecholaminergic polymorphic ventricular tachycardia (CPVT).[7] Mutations have been uncovered in genes encoding subunits of cardiac sodium, potassium and calcium channels, as well as in genes involved in trafficking or regulation of these channels. Approximately half of the cardiac channel mutation positive SIDS cases involve *SCN5A*.[8]

Na_v channels are multi-subunit protein complexes comprised of pore-forming α subunits and multiple protein partners including regulatory β subunits. Four $Na_v\beta$ subunits have been identified in the human heart. Since 1995, mutations in $Na_v1.5$ have been associated with multiple inherited cardiac diseases, including LQT3, BrS, cardiac conduction defect (CCD), atrial fibrillation (AF), sick sinus syndrome (SSS), atrial standstill, and SIDS.[9] Mutations in sodium channel β-subunits have been directly associated with human cardiac disease only in

the last 4 years.[10–17] Here, we report a novel rare variant in *SCN1Bb* associated with BrS and SIDS, examine the structural association of the gene with both sodium channel current (I_{Na}) and transient outward potassium current (I_{to}) channels, and explore the functional effect of the variant on these two channels as a possible novel mechanism contributing to the phenotype. Our study is the first to demonstrate that the $Na_v\beta1B$ subunit has a structural and functional association with both $Na_v1.5$ and $K_v4.3$ and that a genetic variation in this subunit can further modulate I_{Na} and I_{to} so as to modulate the arrhythmogenic substrate responsible for BrS and SIDS.

METHODS

Subjects

The study was conducted in conformance with the guidelines established by the local Human Review Board; written informed consent was obtained from all participants. Genomic DNA from the index cases was extracted from peripheral blood lymphocytes using a commercial kit (Gentra System, Puregene, Valencia, Calif). DNA from 476 patients clinically diagnosed with BrS or SIDS who were genotype-negative for variations in BrS1-4-susceptibility genes (317 males/159 females; 376 Caucasian; age at diagnosis, 6 hours to 72 years) were included in the study and screened for *SCN1B* variants. Control DNA collected from 807 healthy Caucasian subjects was screened for the *SCN1Bb*-R214Q mutations.

Genetic Analysis

Comprehensive open reading frame/splice site genetic analysis was performed using polymerase chain reaction (PCR), denaturing high performance liquid chromatography (DHPLC), and direct DNA sequencing. (See online supplement, including Online Table 1, for details)

Site-Directed Mutagenesis, Transfection and Electrophysiology Study

The ion channel variants were cloned by site-directed mutagenesis, expressed in TSA201 cells and studied using whole cell patch clamp techniques as detailed in the online supplement and reference.[13]

Co-immunoprecipitation and Western Blot

To identify the protein interaction of $Na_v\beta1b$ with $Na_v1.5$ or $K_v4.3$, we used co-immunoprecipitation and western blot assay in plasma membrane of TSA201 cells. (See online supplement)

RESULTS

Clinical History

Patient 1 was a 44 year old male of European descent presenting because of a suspected Brugada ECG at baseline (Figure 1A). His medical history was unremarkable. The patient denied syncope or palpitations. There was no family history of SCD or syncope. Prominent ST segment elevation was induced in leads V1 and V2 following administration of 40 mg of ajmaline confirming the diagnosis of BrS (Figure 1A, upper panel; Online Table 2). The coved-type ST segment elevation was also documented to occur spontaneously during repetitive ECG recordings obtained during follow-up. Electrophysiological study revealed normal AV conduction (AH interval 104 ms and HV 44 ms). Wenckebach cycle length was achieved at a cycle length of 320 ms and sinus node recovery time was also normal (920 ms). Dual AV node physiology was seen without induction of atrioventricular nodal

reentrant tachycardia (AVNRT). Ventricular fibrillation (VT) was inducible with two extrastimuli applied to the right ventricular outflow tract (RVOT) (Figure 1A, lower panel). An implantable cardioverter-defibrillator (ICD) was implanted for primary prevention; no shocks have been reported during follow-up.

Patient 2 was a 62 y/o female, who had cardiac arrest after developing diarrhea and fever. Echocardiography was normal. Two months after the cardiac arrest, the ECG exhibited a typical coved-type ST segment elevation in leads V1-V2 consistent with BrS. Atrioventricular (AV) conduction was within the normal range (Figure 1B, Online Table 2). She had significant neurological sequelae and, therefore, was not implanted with an ICD. Her maternal aunt died from SCD at the age of 19 y/o; and her son is asymptomatic with normal ECG. Unfortunately DNA was not available for the aunt who died suddenly and the son refused genetic testing.

Patient 3 was a Caucasian female from Mayo Clinic SIDS database who died at 4 months of age. An ECG was not available.

Molecular Genetics

Of the genotype-negative probands, 184 cases diagnosed with BrS and 292 cases diagnosed with SIDS were screened for *SCN1B* variations, three were identified with the same variation in exon 3A of *SCN1Bb*. PCR-based sequencing analysis revealed a double peak in the sequence of *SCN1Bb* (Figure 2A) showing a G-to-A transversion at nucleotide 641, predicting a substitution of Glutamine (Q) for Arginine (R) at residue 214 (designated R214Q or p.Arg214Gln). This nucleotide change was observed in 4 of 807 controls (frequency, 0.50%); a frequency of 0.20% is reported in the 1000 genome project database (rs 66876876). The N-terminal region of the human *SCN1Bb* subunit is encoded by exons 1–3, whereas the novel C-terminal region is encoded via the extension of exon 3 to intron 3 (or partial intron 3 retention) with an in-frame stop codon. As the site of divergence between the *SCN1B* and *SCN1Bb* subunit cDNAs was located precisely at the exon 3/intron 3 boundary of the *SCN1B* gene, the human *SCN1Bb* is considered to be a splice variant of the *SCN1B*. R214 is located in exon 3A, and in the extra cellular domain (ECD) of *SCN1Bb* (Figure 2B and 2C). The 3 probands positive for *SCN1Bb*/R214Q were negative for the other candidate genes. All R214Q-positive cases also had the following non-synonymous heterozygous variants: L210P, S248Rand R250T, which had frequencies of 44%, 22% and 22%, respectively.

Electrophysiological characteristics of *SCN5A* co-expressed with *SCN1Bb*/wild-type (WT) and *SCN1Bb*/R214Q

SCN5A/WT, *SCN5A*/WT+*SCN1Bb*/WT, and *SCN5A*/WT+*SCN1Bb*/R214Q were expressed in TSA201 cells to assess the effects of the rare variant on I_{Na} function. Figure 3 shows macroscopic currents recorded from these channels, together with the current-voltage (I-V) relationships. No shift was observed in the maximum peak inward current voltage for any of the channel types. Co-expression of *SCN1Bb*/WT with *SCN5A*/WT increased peak I_{Na} density from −267.33±64.59 pA/pF to −472.60±77.09 pA/pF (n=9 and 11, respectively; $P<0.05$). Co-expression of SCN1Bb/R214Q resulted in a peak I_{Na} current density of −205.70+-57.74 pA/pF (n=12), 56.5% smaller than SCN5A/WT+SCN1Bb/WT and 33.05% smaller than SCN5A/WT (P<0.05; Figure 3B and 3C).

We fitted the decay of the current to the sum of 2 exponentials. At a potential of −20 mV, the time constants of the fast and slow component (τ_s and τ_f) of the current decay were similar among the 3 groups (Figure 4).

Figure 5 shows the results of steady-state activation and inactivation. No difference was observed in half-inactivation voltage ($V_{1/2}$) or slop factor (k) between mutant I_{Na} channels and the 2 WT groups (Figure 5A and 5B). Steady-state activation was also similar among the 3 groups (Figure 5C). The results of recovery from inactivation, measured using a standard double paired-pulse protocol, are shown in Figure 5D. *SCN5A*/WT+*SCN1Bb*/WT had similar τ_f, but faster τ_s (P<0.05) compared with *SCN5A*/WT. Both τ_f and τ_s were slower in *SCN5A*/WT+*SCN1Bb*/R214Q compared with *SCN5A*/WT+*SCN1Bb*/WT (P<0.05 respectively; Figure 5D). R214Q caused no significant shift in the voltage–dependence of steady-state inactivation and activation, but decelerated recovery from inactivation, thus serving to further reduced sodium channel availability (see details in Online Table 3).

Electrophysiological characteristics of *KCND3* co-expressed with WT and mutant *SCN1Bb*

In light of the demonstration by Deschenes et al.[18] of an effect of *SCN1B* to modulate Kv4.3 current, we sought to examine the hypothesis that *SCN1Bb* has a similar effect and that this action of the auxiliary subunit may be amplified by the rare variant. At +40 mV and +80 mV, co-expression of *SCN1Bb*/WT with *KCND3*/WT increased I_{to} density by approximately 64.59% and 66.17% (P<0.05 and P<0.01) over *KCND3*/WT; co-expression of *SCN1Bb*/R214Q with *KCND3*/WT enhanced the I_{to} density further (increasing by 173.51% and 183.55% over *KCND3*/WT current, P<0.01 respectively; and by 66.17% and 70.64% over *KCND3*/WT+*SCN1Bb*/WT current, P<0.01 respectively; Figure 6A and 6C). *SCN1Bb*, both WT and rare variant, did not alter the I-V relationship compared with *KCND3*/WT (Figure 6B), steady-state inactivation (Figure 7C and Online Table 4) or time to peak (Figure 7D), but significantly affected the other kinetics and voltage dependence of channel gating compared to *KCND3*/WT alone.

The effect of *SCN1Bb*/WT and *SCN1Bb*/R214Q on recovery of I_{to} from inactivation is shown in Figure 7A. τ_f with *SCN1Bb*/WT was slightly slower than *KCND3*/WT alone; τ_f and τ_s with co-expression of the *SCN1Bb*/R214Q were significantly slower as compared with two WT groups (Figure 7B and Online Table 4). A double-exponential function was fitted to the current decay of traces elicited by pulses from 0 mV to +80 mV. Figure 7E and 7F show inactivation time constants (τ_f and τ_s) for I_{to} at various potentials. *KCND3*/WT channel inactivation kinetics were faster at the more positive potentials (τ_f and τ_s decreased from 64.76 ± 2.55 ms and 396.53 ± 23.37 ms at 0 mV to 45.35 ± 2.05 ms and 204.85 ± 14.99 ms at +40 mV; n = 33). Co-expression of *SCN1Bb*/WT produced a moderate acceleration of inactivation as reflected by the slightly smaller time constant at all test potentials (P<0.05 for τ_f between +60 mV to +80 mV; P<0.05 for τ_s between +50 mV to +80 mV). With co-expression of *SCN1Bb*/R214Q, inactivation kinetics were slower compared to *KCND3*/WT alone (P<0.05 for τ_s between +60 mV to +80 mV) and *KCND3*/WT+*SCN1Bb*/WT (P<0.05 for τ_f and τ_s between 0 mV to +80 mV). Because co-expression of *SCN1Bb*/R214Q produces both an increase in peak current and a deceleration of current decay, we calculated the change in total charge contributing to the early phases of the action potential (AP). Figures 6D and 6E show that, compare with *KCND3*/WT and *KCND3*/WT +*SCN1Bb*/WT, there is a statistically significant increase in total charge during the first 50 and 100 ms of *KCND3*/WT+ *SCN1Bb*/R214Q current.

Co-immunoprecipitation Study

To determine whether *SCN1Bb* proteins associate with *KCND3*, we prepared extracts of TSA201 cells transfected with *SCN1Bb* and *SCN5A*, or *SCN1Bb* and *KCND3* (n = 4). Figure 8A and 8B display western blots of the immunoprecipitated proteins showing a ~30 kDa *SCN1Bb* band using the anti-*SCN1Bb* antibody. These results provide evidence in

support of an interaction of subsidiary *SCN1Bb* subunits (both WT and rare variant) with *SCN5A* and *KCND3* subunits in the transfected cells.

DISCUSSION

Mutations in *SCN1B* have recently been associated with AF and CCD and two stop-codon mutations in *SCN1Bb* have been associated with a BrS/CCD (Online DISCUSSION and Online Table 5). In the present study, we identified a novel genetic variant in *SCN1Bb* in with BrS and SIDS, which is the first missense rare variant in *SCN1Bb* gene related to cardiac disease. In patient 1, VF was induced with programmed stimulation applied to the RVOT. In the case of patient 2, aborted SCD occurred in conjunction with diarrhea and fever, previously reported triggers,[19, 20] and generally associated with *SCN5A*-mediated BrS.[21] No mutation in *SCN5A* was found in this patient. The identification of the variant in patient 3 expands the spectrum of channelopathies associated with SIDS and provides further support for our hypothesis that, infants having rapid ventricular tachycardia, conduction abnormalities, (aborted) sudden death in the absence of structural or metabolic abnormalities are likely to have disease-causing genetic variants in cardiac depolarizing channels, including sodium and calcium channels.[22]

The *SCN1Bb* gene, which encodes a splice variant of $Na_v\beta1$ subunit (termed $Na_v\beta1B$), is located on chromosome 19 (19q13.1-q13.2). A 268 residue protein, with a calculated molecular mass of 30.4 kDa, is encoded by 807 bp open reading frame of the human $Na_v\beta1B$ subunit.[23] It is formed through retention of intron 3, containing a stop codon. The predicted amino acid sequence of the retained intronic region exhibits very low homology between species, and the C-terminal region of the human $Na_v\beta1B$ is significantly different from that of the $Na_v\beta1$ and $Na_v\beta1A$ subunits. The rare variant of c.641G>A in exon 3A results in substitution of a polar glutamine for a basic arginine at position 214. It is located at the ECD, which interacts with $Na_v1.5$, and has been shown to be both necessary and sufficient for the modulation of Na+ channel characteristics.[24]

$Na_v\beta$ subunits have been proposed to exert multiple influences on function of the human $Na_v1.5$, including altered activation, inactivation and recovery from inactivation; altered channel expression at the plasma membrane; as well as modulation of other related proteins in the cardiac sodium complex. Moreover, β-subunits modify not only the biophysical, but also the pharmacological properties of the cardiac sodium channel complex.[25] Compared with those of other subunits, $Na_v\beta1$-mediated effects on $Na_v1.5$ are the most investigated.[26] Expression of $Na_v1.5$ in oocytes produces channels that inactivate rapidly in the absence of $Na_v\beta$ subunits.[27] According to some reports, $Na_v\beta1$ has no observable effect on *SCN5A* function.[28] Most other groups have reported a $Na_v\beta1$-dependent increase in I_{Na} amplitude. No detectable effects on channel kinetics or voltage-dependence are observed by several groups.[29] A number of studies have reported a $Na_v\beta1$-mediated 5–15mV depolarizing shift of steady-state inactivation,[26, 30] or significant changes in the rate of recovery from inactivation.[30] Makielski and co-workers reported modulation of channel sensitivity to lidocaine block with subtle changes in channel kinetics and gating properties in response to $Na_v\beta1$ expression.[31] As the majority of these studies focusing on Navβ1, similar studies have not been carried out for Navβ1B. In the present study, we demonstrate that $Na_v\beta1B$/WT increases $Na_V1.5$ density, consistent with previous studies conducted using CHO cells[11] or Oocytes.[23] The R214Q rare variant in $Na_v\beta1B$ blunted or inhibited the gain of function produced by $Na_v\beta1B$/WT on I_{Na} density.

I_{to}, encoded by Kv4 family of potassium channels, is responsible for phase 1 of the AP. Recent studies indicate that co-expression of the $Na_v\beta1$ subunit modulates the gating properties of Kv4.3 to closely recapitulate native I_{to},[18] and plays a key role in the structural

association between subunits that comprise the I_{to} and I_{Na} channels.[32] Coimmunoprecipitation studies revealed association of $K_v4.2$ or $K_v4.3$ with $Na_v\beta1$ in ventricular myocardium. Inhibition of $Na_v\beta1$ transcription in ventricular myocytes results in the reduction of mRNA and/or protein levels of $Na_v1.5$, $K_v4.2$, $K_v4.3$, and KChIP2, and the marked decrease in I_{Na} and I_{to}. Together, these intriguing observations suggest that cardiac $Na_v1.5$ may physically associate with I_{to} channels via β1 to form a macromolecular complex. Here, we first describe that Navβ1B subunit has a similar structural and functional association with $hK_v4.3$, including co-localization with $hK_v4.3$ protein and a gain of function of $I_{to.}$ The increase in Kv4.3 current effected by co-expression of *SCN1Bb*/WT appears less significant than that of *SCN1B*/WT reported by Deschênes et al.[18] Our study is the first to demonstrate that a rare genetic variant in $Na_v\beta$ subunit can produce a gain of function in $hK_v4.3$ channel current. The R214Q variation in $Na_v\beta1B$ caused a prominent further augmentation of total charge due to an increase in I_{to} density and a slowing of the rate of inactivation. The remarkable gain in function of I_{to} likely contributes importantly to development of both the BrS and SIDS phenotypes. The combination of an increase in I_{to} and decrease in I_{Na} is expected to produce a prominent outward shift in net current active during the early phases of the epicardial AP, particularly in right ventricular epicardium where I_{to} is generally more prominent. This in turn would lead to accentuation of the right ventricular epicardial AP dome, heterogeneous loss of the AP dome, giving rise to phase 2 reentry and polymorphic VT.

The intracellular domain of β1 is critical for Na_v1-ankyrin (G and B) interaction and channel modulation *in vitro.*[33] In addition, $Na_v1.5$ channels of the intercalated disk-pool were shown to not only co-localize with phosphotyrosin-β1, but also with connexin-43 (a well-known intercalated disk protein) and N-cadherin.[34, 35] It has been suggested that mutations in $Na_v\beta1$ may also disrupt channel-cytoskeletal interactions. The effect of $Na_v\beta1B$ (WT and R214Q) on other proteins may also plays a role in human health and disease. This crosstalk between $Na_v\beta1$/$Na_v\beta1B$ and other proteins is an encrypted language that remains to be deciphered. (See more discussion in online supplement)

Limitations

Our data indicate that *SCN1Bb*/R214Q is a functional rare variant that occurs in all our patients together with 3 very common polymorphisms. The degree to which *in vitro* characteristics might be altered in the context of these polymorphisms is not known and will require further investigation. It is noteworthy that although the R214Q variant was not detected among 354 ethnically-matched healthy controls tested in Utica, NY, USA or Pavia, Italy, it was found in 4 of 453 presumably healthy controls tested in Rochester, Minn, USA (ECGs or clinical history not available). We are obliged to conclude that this variant may not be greatly over-represented in BrS or SIDS cases.

CONCLUSION

In summary, our study is the first to demonstrate that the $Na_v\beta1B$ subunit has a structural and functional association with both $Na_v1.5$ and $K_v4.3$ and that a genetic variation in this subunit may further modulate I_{Na} and I_{to} so as to functionally modulate the expression of a BrS phenotype in adults as well as an arrhythmogenic substrate responsible for SIDS. Our study provides evidence in support of the hypothesis that a rare variant in the $Na_v\beta1B$ subunit leading to augmentation of net outward current via concomitant reduction in inward current and increase in outward current constitutes another mechanism contributing to the development of a BrS and SIDS phenotypes.

Supplementary Material

Refer to Web version on PubMed Central for supplementary material.

Acknowledgments

The authors are grateful to Judy Hefferon, Robert J. Goodrow, Susan Bartkowiak, Margherita Torchio, Rebellato Luca, Federica Dagradi, MD and Silvia Castelletti, MD for technical assistance.

FUNDING SOURCES

This work was supported by a grant HL47678 from NHLBI, grants from NYSTEM, the Masons of New York State and Florida for CA. Supported by the Mayo Clinic Windland Smith Rice Comprehensive Sudden Cardiac Death Program and the NIH, USA (HD42569) for MJA. Supported by MICINN grant (SAF2010-16120/) for OC.

ABBREVIATIONS

AF	atrial fibrillation
AP	action potential
AV	atrioventricular
AVNRT	atrioventricular nodal reentrant tachycardia
BrS	Brugada syndrome
CCD	cardiac conduction defect
CPVT	catecholaminergic polymorphic ventricular tachycardia
CAMs	cellular adhesion molecules
DHPLC	denaturing high performance liquid chromatography
ECD	extracellular domain
ERS	early repolarization syndrome
ICD	implantable cardioverter-defibrillator
LQTS	long QT syndrome
PCR	polymerase chain reaction
RVOT	right ventricular outflow tract
SQTS	short QT syndrome
SSS	sick sinus syndrome
$\mathbf{I_{Na}}$	sodium channel current
SCD	sudden cardiac death
SIDS	sudden infant death syndromes
$\mathbf{I_{to}}$	transient outward potassium current
VT/VF	ventricular tachycardia/ventricular fibrillation
WT	wild type

References

1. Antzelevitch C. Brugada syndrome. PACE. 2006; 29:1130–59. [PubMed: 17038146]
2. Antzelevitch C, Yan GX. J wave syndromes. Heart Rhythm. 2010; 7:549–58. [PubMed: 20153265]

3. Burashnikov E, Pfeiffer R, Barajas-Martinez H, et al. Mutations in the cardiac L-type calcium channel associated J wave sydnrome and sudden cardiac death. Heart Rhythm. 2010; 7:1872–82. [PubMed: 20817017]
4. Giudicessi JR, Ye D, Tester DJ, et al. Transient outward current (Ito) gain-of-function mutations in the KCND3-encoded Kv4.3 potassium channel and Brugada syndrome. Heart Rhythm. 2011; 8:1024–32. [PubMed: 21349352]
5. Kattygnarath D, Maugenre S, Neyroud N, et al. MOG1: a new susceptibility gene for Brugada syndrome. Circ Cardiovasc Genet. 2011; 4:261–8. [PubMed: 21447824]
6. Van Norstrand DW, Ackerman MJ. Genomic risk factors in sudden infant death syndrome. Genome Med. 2010; 2:86. [PubMed: 21122164]
7. Tester DJ, Ackerman MJ. Sudden infant death syndrome: how significant are the cardiac channelopathies? Cardiovasc Res. 2005; 67:388–96. [PubMed: 15913580]
8. Arnestad M, Crotti L, Rognum TO, et al. Prevalence of long-QT syndrome gene variants in sudden infant death syndrome. Circulation. 2007; 115:361–7. [PubMed: 17210839]
9. Remme CA, Wilde AA, Bezzina CR. Cardiac sodium channel overlap syndromes: different faces of *SCN5A* mutations. Trends Cardiovasc Med. 2008; 18:78–87. [PubMed: 18436145]
10. Watanabe H, Darbar D, Kaiser DW, et al. Mutations in sodium channel b1 and b2 subunits associated with atrial fibrillation. Circ Arrhythm Electrophysiol. 2009; 2:268–75. [PubMed: 19808477]
11. Watanabe H, Koopmann TT, Le Scouarnec S, et al. Sodium channel b1 subunit mutations associated with Brugada syndrome and cardiac conduction disease in humans. J Clin Invest. 2008; 118:2260–8. [PubMed: 18464934]
12. Olesen MS, Jespersen T, Nielsen JB, et al. Mutations in sodium channel {beta}-subunit SCN3B are associated with early-onset lone atrial fibrillation. Cardiovasc Res. 2011; 89:786–93. [PubMed: 21051419]
13. Hu D, Barajas-Martinez H, Burashnikov E, et al. A mutation in the beta 3 subunit of the cardiac sodium channel associated with Brugada ECG phenotype. Circ Cardiovasc Genet. 2009; 2:270–8. [PubMed: 20031595]
14. Tan BH, Pundi KN, Van Norstrand DW, et al. Sudden infant death syndrome–associated mutations in the sodium channel beta subunits. Heart Rhythm. 2010; 7:771–8. [PubMed: 20226894]
15. Valdivia CR, Medeiros-Domingo A, Ye B, et al. Loss-of-function mutation of the SCN3B-encoded sodium channel b3 subunit associated with a case of idiopathic ventricular fibrillation. Cardiovasc Res. 2010; 86:393–400.
16. Wang P, Yang Q, Wu X, et al. Functional dominant-negative mutation of sodium channel subunit gene SCN3B associated with atrial fibrillation in a Chinese GeneID population. Biochem Biophys Res Commun. 2010; 398:98–104. [PubMed: 20558140]
17. Medeiros-Domingo A, Kaku T, Tester DJ, et al. *SCN4B*-encoded sodium channel b4 subunit in congenital long-QT syndrome. Circulation. 2007; 116:134–42. [PubMed: 17592081]
18. Deschênes I, Tomaselli GF. Modulation of $K_V4.3$ current by accessory subunits. FEBS Lett. 2002; 528:183–8. [PubMed: 12297301]
19. Burrell C, Reddy S, Haywood G, Cunningham R. Cardiac arrest associated with febrile illness due to U.K. acquired Cyclospora cayetanensis. J Infect. 2007; 54:e13–e15. [PubMed: 16684571]
20. Makaryus JN, Verbsky J, Schwartz S, Slotwiner D. Fever associated with gastrointestinal shigellosis unmasks probable Brugada syndrome. Case Report Med. 2009; 2009:492031. [PubMed: 20069106]
21. Dumaine R, Towbin JA, Brugada P, et al. Ionic mechanisms responsible for the electrocardiographic phenotype of the Brugada syndrome are temperature dependent. Circ Res. 1999; 85:803–9. [PubMed: 10532948]
22. Kanter RJ, Pfeiffer R, Hu D, Barajas-Martinez H, Carboni M, Antzelevitch C. Brugada-like syndrome in infancy presenting with rapid ventricular tachycardia and intraventricular conduction delay. Circulation. 2011
23. Qin N, D'Andrea MR, Lubin ML, Shafaee N, Codd EE, Correa AM. Molecular cloning and functional expression of the human sodium channel beta1B subunit, a novel splicing variant of the beta1 subunit. Eur J Biochem. 2003; 270:4762–70. [PubMed: 14622265]

24. McCormick KA, Srinivasan J, White K, Scheuer T, Catterall WA. The extracellular domain of the beta1 subunit is both necessary and sufficient for beta1-like modulation of sodium channel gating. J Biol Chem. 1999; 274:32638–46. [PubMed: 10551818]
25. Uebachs M, Opitz T, Royeck M, et al. Efficacy loss of the anticonvulsant carbamazepine in mice lacking sodium channel beta subunits via paradoxical effects on persistent sodium currents. J Neurosci. 2010; 30:8489–501. [PubMed: 20573896]
26. Malhotra JD, Chen C, Rivolta I, et al. Characterization of sodium channel a- and b-subunits in rat and mouse cardiac myocytes. Circulation. 2001; 103:1303–10. [PubMed: 11238277]
27. Qu Y, Isom LL, Westenbroek RE, et al. Modulation of cardiac Na^+ channel expression in *Xenopus* oocytes by b1 subunits. J Biol Chem. 1995; 270:25696–701. [PubMed: 7592748]
28. Yang JS, Bennett PB, Makita N, George AL, Barchi RL. Expression of the sodium channel b1 subunit in rat skeletal muscle is selectively associated with the tetrodotoxin-sensitive a subunit isoform. Neuron. 1993; 11:915–22. [PubMed: 8240813]
29. Nuss HB, Chiamvimonvat N, Perez-Garcia MT, Tomaselli GF, Marban E. Functional association of the b_1 subunit with human cardiac (hH1) and rat skeletal muscle (m1) sodium channel a subunits expressed in *Xenopus* oocytes. J Gen Physiol. 1995; 106:1171–91. [PubMed: 8786355]
30. Ko SH, Lenkowski PW, Lee HC, Mounsey JP, Patel MK. Modulation of $Na_v1.5$ by b1- and b3-subunit co-expression in mammalian cells. Pflugers Arch. 2005; 449:403–12. [PubMed: 15455233]
31. Makielski JC, Limberis JT, Chang SY, Fan Z, Kyle JW. Coexpression of b1 with cardiac sodium channel a subunits in oocytes decreases lidocaine block. Mol Pharmacol. 1996; 49:30–9. [PubMed: 8569709]
32. Deschenes I, Armoundas AA, Jones SP, Tomaselli GF. Post-transcriptional gene silencing of KChIP2 and Navbeta1 in neonatal rat cardiac myocytes reveals a functional association between Na and Ito currents. J Mol Cell Cardiol. 2008; 45:336–46. [PubMed: 18565539]
33. McEwen DP, Meadows LS, Chen C, Thyagarajan V, Isom LL. Sodium channel b1 subunit-mediated modulation of Nav1.2 currents and cell surface density is dependent on interactions with contactin and ankyrin. J Biol Chem. 2004; 279:16044–9. [PubMed: 14761957]
34. Malhotra JD, Kazen-Gillespie K, Hortsch M, Isom LL. Sodium channel beta subunits mediate homophilic cell adhesion and recruit ankyrin to points of cell-cell contact. J Biol Chem. 2000; 275:11383–8. [PubMed: 10753953]
35. Malhotra JD, Thyagarajan V, Chen C, Isom LL. Tyrosine-phosphorylated and nonphosphorylated sodium channel beta1 subunits are differentially localized in cardiac myocytes. J Biol Chem. 2004; 279:40748–54. [PubMed: 15272007]

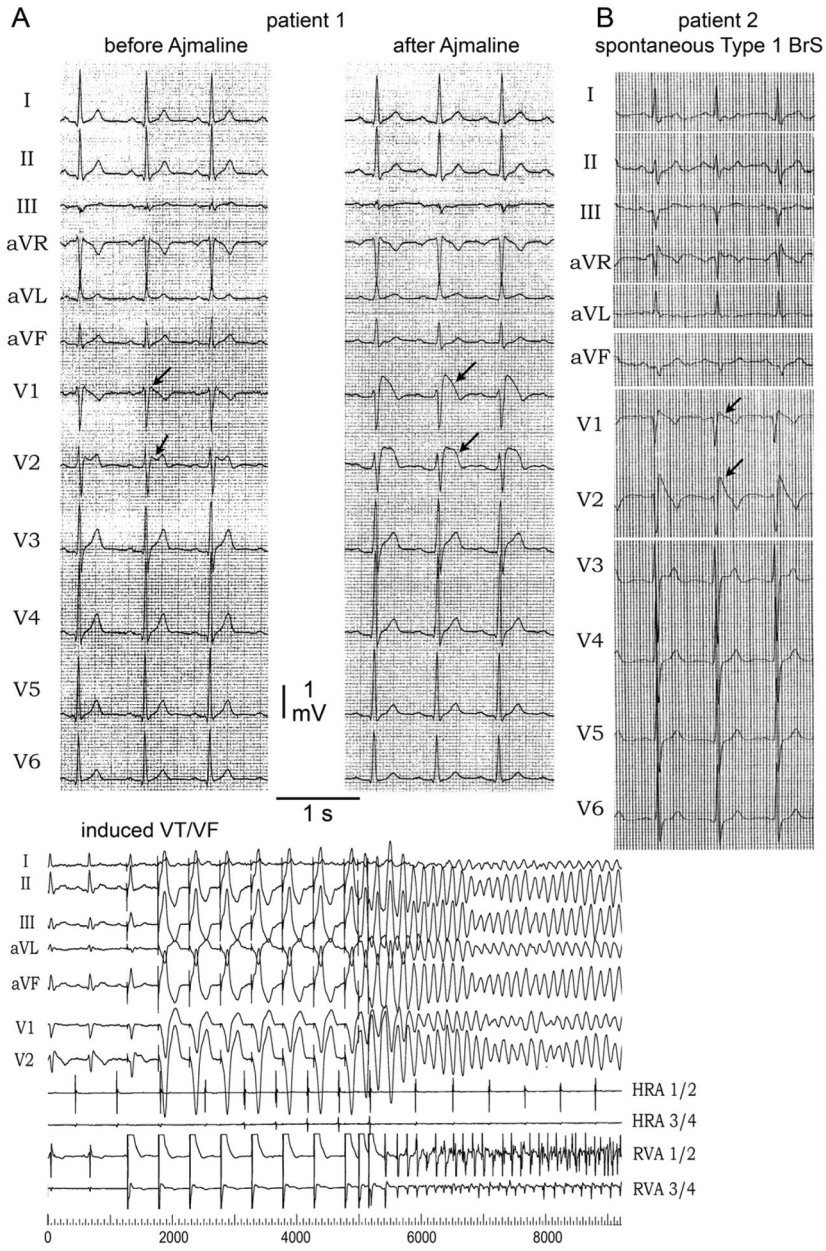

Figure 1. ECG of the patient 1 and patient 2 with Brugada syndrome (BrS) sign

A: (Upper panel) ECG at rest and 10 minutes after 40 mg of Ajmaline in patient 1. After sodium channel block challenge**,** ECG shows accentuation of R′ and development of a type 1 ST segment elevation in V1 and V2 (arrows). **(Lower panel)** Clinical electrophysiology study on patient 1. Ventricular tachycardia/ventricular fibrillation (VT/VF) was inducible with two extrastimulis. **B:** ECG of patient 2. It shows spontaneous huge accentuation of R′ and type 1 ST segment elevation in V1, and V2 (arrows).

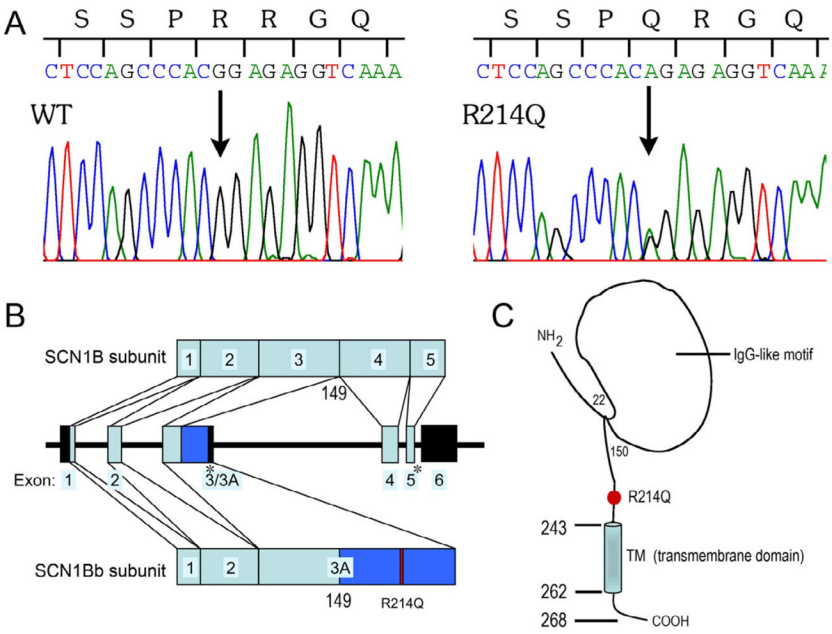

Figure 2. Genetic analysis of *SCB1Bb*/R214Q

A: polymerase chain reaction -based sequence of *SCN1Bb* exon 3A showing wild-type (WT) and heterozygous G to A transversion at nucleotide 641 (arrow). It predicts a substitution of glutamine (CAG) for arginine (CGG) at position 214 (R214Q). **B:** Genomic structure of human Navβ1 gene. On chromosome 19, the *SCN1B* spans around 9 kb across six exons. *SCN1Bb* shares an identical N-terminal half (residues 1–149) with *SCN1B*, but contains a novel C-terminal half of less than 17% sequence identity with *SCN1B*. Exon 3A is an extended exon 3 (retention of part of intron 3) via alternative splicing. The dark blue region indicates the unique sequence of exon 3A compared with exon 3. Exons 1–5 (light blue boxes) encode the Navβ1 subunit, while exons 1, 2 and 3A (light and dark blue boxes) encode the Navβ1B subunit. The stop codon is indicated by an asterisk, the mutation is indicated as red box, and the untranslated regions are indicated using the black boxes. **C:** Predicted topology of Navβ1B. Red circle indicates the location of the mutant.

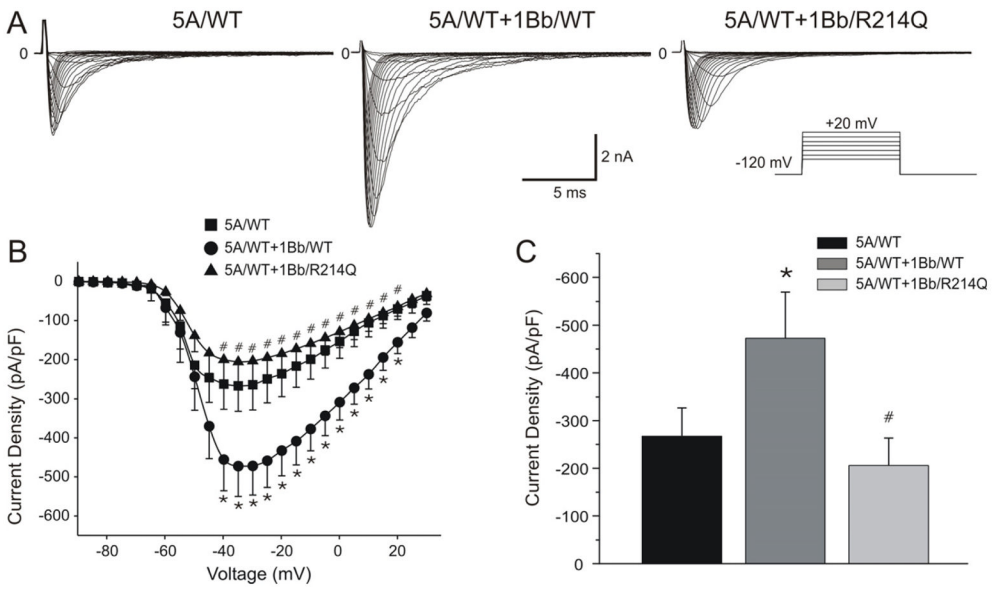

Figure 3. Effect of *SCN1Bb*/R214Q on I_{Na} expressed in TSA201 cells

A: Representative I_{Na} traces in cells expressing *SCN5A*/wild-type (WT) alone or co-transfected with *SCN1Bb*/WT or *SCN1Bb*/R214Q. Co-expression of *SCN1Bb*/R214Q produced loss of function. The inset shows the voltage-clamp protocol employed. **B:** Current-Voltage relationship for *SCN5A*/WT (n=9), *SCN5A*/WT + *SCN1Bb*/WT (n=11) and *SCN5A*/WT + *SCN1Bb*/R214Q (n=12). **C:** Bar graph of peak current density indicated significantly reduced for *SCN5A*/WT and *SCN5A*/WT + *SCN1Bb*/R214Q when compared to *SCN5A*/WT + *SCN1Bb*/WT ($^{*}P<0.05$, compared with *SCN5A*/WT; $^{\#}P<0.05$, compared with *SCN5A*/WT+*SCN1Bb*/WT).

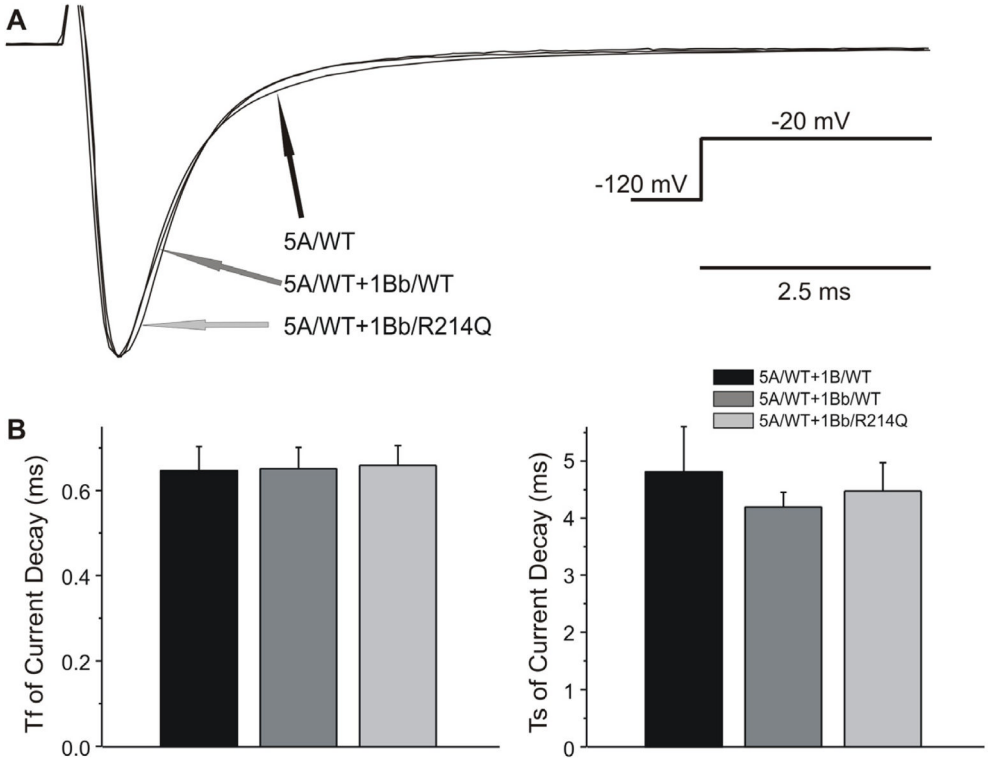

Figure 4. The effect of *SCN1Bb* subunit on current decay of I_{Na}

A: Overlapping sodium channel current (I_{Na}) traces from cells expressing $Na_V1.5$, in the absence and presence of *SCN1Bb* wild-type (WT) and variant. I_{Na} was evoked by +20mV depolarizing pulses from a holding potential of −120m V. Traces are shown normalized to their individual peak value. **B and C:** Current decay (τ_f and τ_s) for all 3 groups fitted with double exponential function.

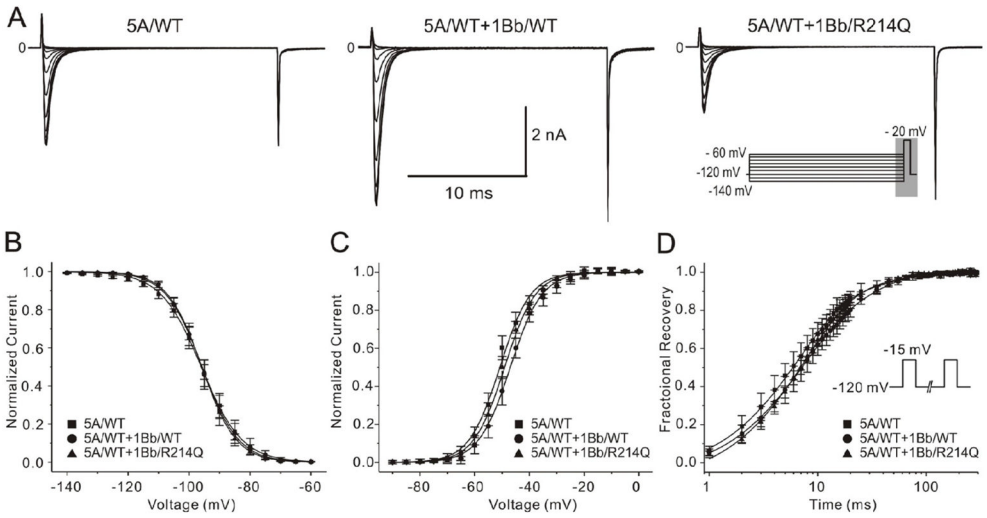

Figure 5. Functional characterization of *SCN1Bb*/R214Q on I_{Na}

A: Representative traces recorded from wild-type (WT) and mutant channels in response to the voltage clamp protocol depicted on right middle inset designed to assess steady-state inactivation. **B and C:** Voltage dependence of inactivation and activation of *SCN5A*/WT and co-transfection of either *SCN1Bb*/WT or *SCN1Bb*/R214Q. Averaged values and the number of cells used are represented in Online Table 3. **D:** Recovery from fast inactivation of 3 groups determined using the two-pulse protocol shown in the inset. Fitting to a double-exponential function yielded the time constants demonstrated in Online Table 3. τ_f and τ_s in *SCN5A*/WT + *SCN1Bb*/R214Q were significantly slower as compared with *SCN5A*/WT + *SCN1Bb*/WT.

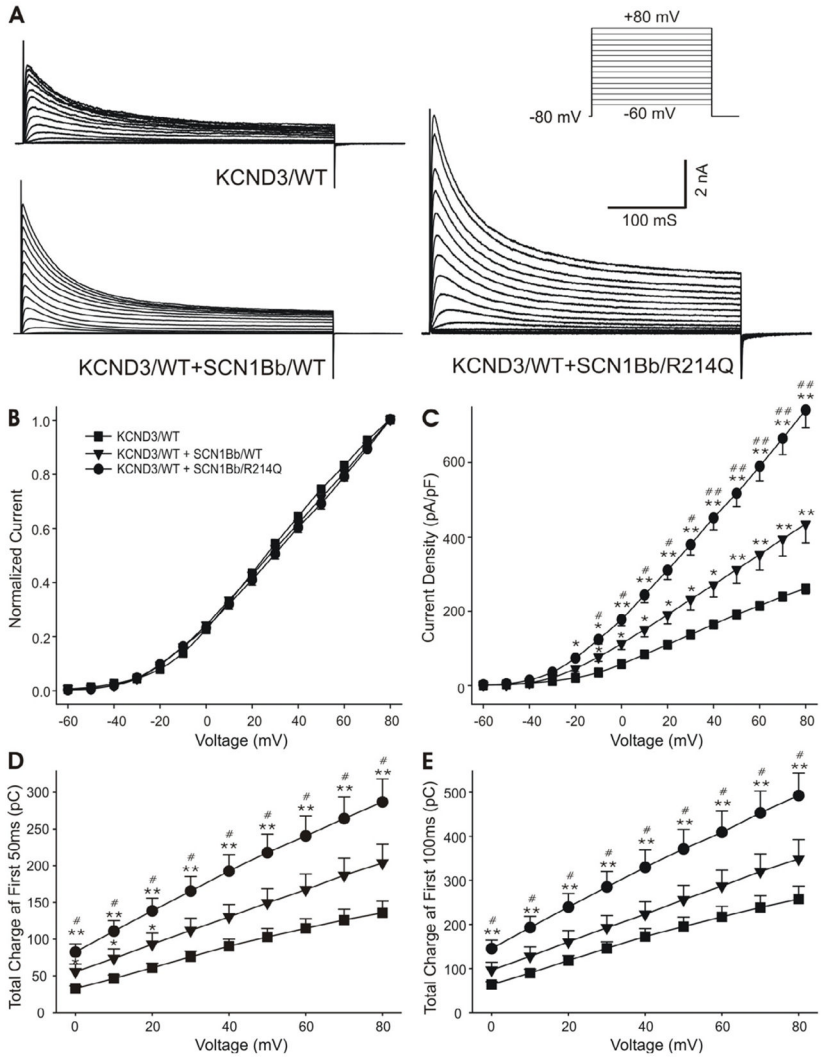

Figure 6. Effect of *SCN1Bb*/R214Q on I_{to}

A: Representative I_{to} traces recorded from cells expressing *KCND3*/wild-type (WT) alone or co-transfected with *SCN1Bb*/WT or *SCN1Bb*/R214Q. Co-expression of *SCN1Bb*/R214Q produced gain of function. The inset shows the voltage-clamp protocol employed. **B:** Normalized current-voltage relationship for *KCND3*/WT, *KCND3*/WT + *SCN1Bb*/WT and *KCND3*/WT + *SCN1Bb*/R214Q. There is no significant change in the presence of *SCB1Bb* (WT/R214Q) compared with both WT groups. **C:** Raw current-voltage relationship for peak I_{to} current density. **D and E**: Total charge of I_{to} current during the first 50 ms and 100 ms as a function of voltage. For panel B–E: n=31, 10, 11 for *KCND3*/WT, *KCND3*/WT + *SCN1Bb*/WT, *KCND3*/WT + *SCN1Bb*/R214Q; $^{*}P<0.05$, $^{**}P<0.01$ compared with KCND3/WT; $^{\#}P<0.05$, $^{\#\#}P<0.01$ compared with *KCND3*/WT+*SCN1Bb*/WT.

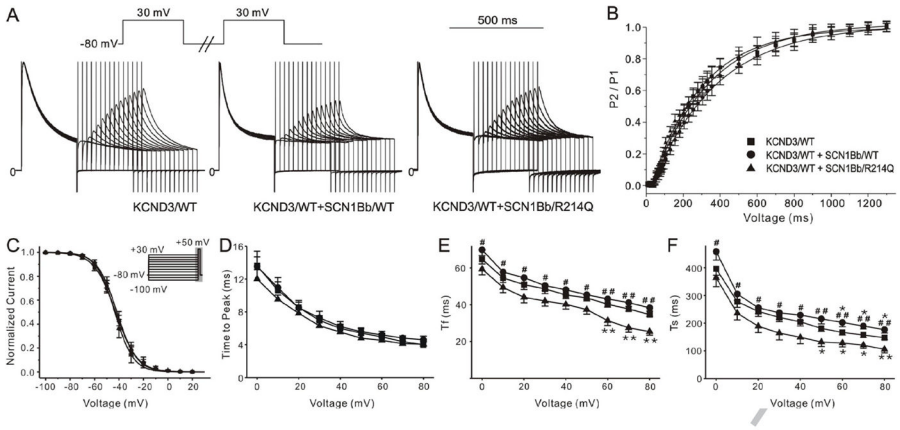

Figure 7. Functional characterization of *SCN1Bb*/R214Q on I_{to}

A: Representative traces recorded from wild-type (WT) and mutant channels in response to the voltage clamp protocol depicted on the top left inset designed to assess recovery. P1 was normalized to the same amplitude. **B:** Recovery from inactivation of 3 groups. **C:** Voltage dependence of inactivation of *KCND3*/WT and co-transfection of either *SCN1Bb*/WT or *SCN1Bb*/R214Q. The protocol was displayed in the top inset of Figure 7C. Averaged values and the number of cells used are represented in Online Table 4. **D**: Time to peak current as a function of voltage. **E and F:** Kinetics of current decay (τ_f and τ_s) for all 3 groups fitted with double exponential function. $^{*}P<0.05$, $^{**}P<0.01$ compared with KCND3/WT; $^{\#}P<0.05$, $^{\#\#}P<0.01$ compared with *KCND3*/WT+*SCN1Bb*/WT.

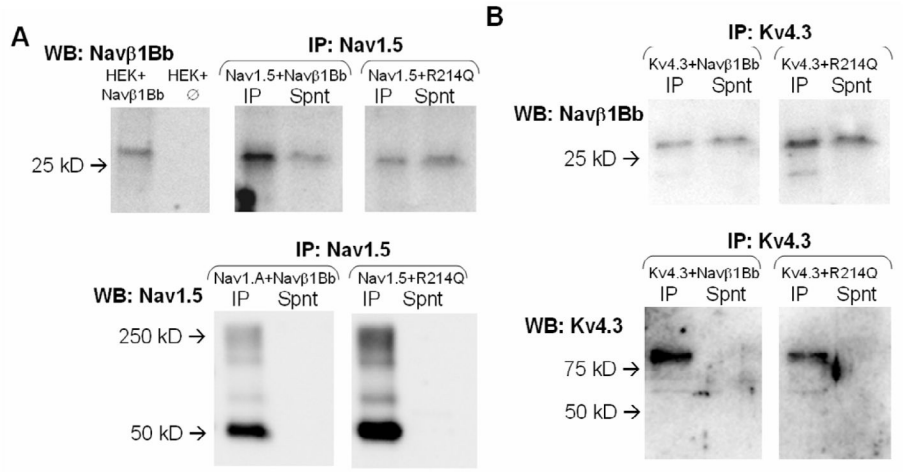

Figure 8. Coimmunoprecipitation of *Nav1.5/Kv4.3* and *Navβ1b* subunit

Proteins were immunoprecipitated with (**A**) anti-*Nav1.5* or (**B**) anti-*Kv4.3* and immunoblotted with anti-*Navβ1b* (WT or R214Q variant) as indicated. Parallel western blot analysis of transfected and untransfected TSA201 cells was performed to confirm identity of labelled bands. Lower panels show that *Nav1.5* and *Kv4.3* are indeed fully precipitated. In both cases, the *Navβ1b* subunit appears in the pellet (IP) and in the supernatant (Spnt) of the immunoprecipitate. Each blot is representative of 4 experiments conducted under the same conditions.